

Dynamical simulation of liquid- and solid-metal self-sputtering

W. Lowell Morgan^{a)}

Joint Institute for Laboratory Astrophysics, National Bureau of Standards and University of Colorado,
Boulder, Colorado 80309

(Received 12 January 1988; accepted for publication 4 October 1988)

Molecular dynamics simulations of self-sputtering are performed using the recent picture [M. P. D'Evelyn and S. A. Rice, *J. Chem. Phys.* **78**, 5081 (1983)] of a stratified liquid-metal surface as a model. These results are compared to those obtained from a liquid model having uniformly distributed atoms and a crystalline solid model. The stratified liquid-metal model shows an enhanced low-energy sputter yield, which falls below those of the other models for ion-impact energies above several hundred electron volts. These results are discussed in light of various published measurements of sputter yields of metals in their liquid and solid phases.

I. INTRODUCTION

It is of scientific interest as well as of some practical interest to understand and be able to model the collisions of atoms with liquid-metal surfaces. A factor that may be important in determining the sticking coefficient for metal atoms incident upon a liquid-metal surface as well as the angular distribution for reflected atoms and sputtering yields and distributions is the topology of the liquid surface. Recent research on the structure of liquid-metal surfaces has shown that these surfaces are likely *not* to be sharp boundaries, with the transition from liquid to vapor (the 90%–10% density points) occurring over two atomic diameters as it does for, say, liquid argon. Instead, theoretical studies^{1–3} and experimental grazing-incidence x-ray determination of the reflectance⁴ and of the structure factor^{5,6} at the liquid-vapor interface indicate a stratification in the density over a number of atomic diameters near the interface.

This structure in the density profile $\rho(z)$, where z is the direction normal to the surface, arises because of the variation in the effective interatomic interactions near the liquid-metal surface. These interatomic forces are strongly dependent upon the density of conduction electrons, which screen the ions. The rapid change in density near the surface and the associated change in electronic potential give rise to oscillations in the electron density, leading to oscillations in the ion density.⁷

In this paper I describe molecular dynamics computer simulations of collisions of low-energy atoms with model stratified liquid, uniformly distributed liquid, and single-crystal solid surfaces of the same bulk density. Of interest is the comparison of sputtering yields and reflectances for the three surfaces, which represent two models for liquid surfaces and a model for a perfect solid surface. My model of the liquid-metal surface follows directly from the work of D'Evelyn and Rice¹ on liquid mercury. There have been previous simulations of sputtering of liquid metals^{8,9} but they used the standard picture of the density profile at a liquid-gas interface, which I have called a uniform liquid

model in my simulations. Although there are no experimental data for sputtering of mercury and scanty data in general for liquid metal sputtering, we will see that the results of this modeling are consistent with most of the published data. These calculations illustrate an interesting and, for some applications, important effect and serve as a prediction for future measurements.

II. SIMULATING ATOMIC COLLISIONS WITH LIQUID-METAL SURFACES

A. Surface structure of liquid mercury

Although this is a study of the sputtering characteristics of model systems, I have drawn on the research of D'Evelyn and Rice¹ on mercury for the stratified liquid-metal model. In modeling the interfacial region of mercury D'Evelyn and Rice defined two types of Hg: metallic and vapor with the metal-nonmetal transition setting in at a density ρ_{mn} of 9–10 g/cm³. The pair interactions in the metallic region are described by a density-dependent effective potential, $\varphi_{\text{eff}}(r; n)$, while those in the vapor region interact via an atomic potential $\varphi_{\text{vap}}(r)$. The atomic potential is purely repulsive, although vapor atoms interact with the conduction electrons in the metal zone via an attractive van der Waals type of potential, $V_s(z_m)$, where z_m is the distance to the metal-like zone. The effective potential in the metallic zone was obtained from pseudopotential calculations which were then adjusted, based on Monte Carlo simulations, to give good agreement with measured pair correlation functions in bulk mercury.

D'Evelyn and Rice then performed extensive equilibrium Monte Carlo (EMC) simulations of the interface region to obtain the density profile for liquid mercury. They fitted their EMC results for $\rho(z)$ with a seven parameter function,

$$\rho(z) = \frac{\rho_b [1 + \{A \sin(2\pi z/\lambda)/(1 + z^2/l^2)\}]}{1 + \exp(z/\delta)} + h \exp\left(-\frac{(z - \xi)^2}{w^2}\right), \quad (1)$$

where $\rho_b = 13.538 \text{ g cm}^{-3}$ ($n = 4.37 \times 10^{-2} \text{ \AA}^{-3}$) is the bulk Hg density.

I have used the above expression for the density profile $\rho(z)$ to generate a model surface for use in dynamics simula-

^{a)} 1987–88 JILA Visiting Fellow. Permanent address: Department of Chemistry and Materials Science, Lawrence Livermore National Laboratory, Box 808 L-446, Livermore, CA 94550.

tions. The values of the constants used are $A = 0.8$, $h = 0.6$, $\zeta = 3.0 \text{ \AA}$, $w = 0.8 \text{ \AA}$, $\delta = 0.6 \text{ \AA}$, $\lambda = 3.0 \text{ \AA}$, and $l = 6.7 \text{ \AA}$. The density profile $\rho(z)$ is shown in Fig. 1. In Fig. 2 is shown a side view of the 900-atom "slab" used in the MD simulations. This represents a snapshot of the spatial distribution of metal atoms for $z \geq -10 \text{ \AA}$ at an instant in time. The unit cell is 36 \AA square in the x - y plane and the bottommost atoms in the metallic zone are at $z = -15 \text{ \AA}$. With the appropriate potentials a dynamical simulation would allow the atoms to move around in thermal motion yet retain the same density profile, $\rho(z)$, as given by the equation above.

B. Interatomic potentials

In performing the dynamical simulations described below, I used a modified Lennard-Jones potential for the interaction between atoms in the slab and a potential function given by D'Evelyn and Rice¹ for the interaction between the incident atom and the slab atoms. Although most sputtering experiments involve collisions between ions and surfaces, I have assumed, following the theory of Hagstrum,^{10,11} that at these low energies metal ions, such as mercury, are likely to have been neutralized by resonant tunneling or Auger processes before colliding with the metallic surface.

The metallic potential used by D'Evelyn and Rice, which was not an analytic function but was tabulated for their calculations, is strongly repulsive having its minimum at an interatomic separation of 4.60 \AA . In a molecular dynamics simulation, however, this potential was not satisfactory in that it did not yield a negative total energy for a liquid at the density of Hg. I found that a potential with a minimum at smaller r , similar to that obtained by Kuroha and Suzuki¹² from pseudopotential calculations, did make the model system stable on the time scale of the collisional and sputtering processes. On a longer time scale, using this potential function, the stratified liquid slab equilibrates to an amorphous slab of uniform density. The potential that I used was a modified Lennard-Jones function,

$$V(r) = -4\epsilon[(\sigma/r)^{12} - \lambda(\rho)(\sigma/r)^6]. \quad (2)$$

The well depth $\epsilon = 0.1 \text{ eV}$ gives approximately the correct cohesive energy and the distance parameter $\sigma = 2.08 \text{ \AA}$ comes from the average nearest-neighbor distance as evidenced by the radial distribution function $g(r)$ for the liquid.

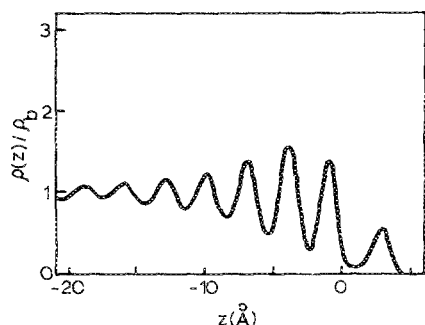


FIG. 1. Model density profile relative to the bulk density near liquid Hg surface.

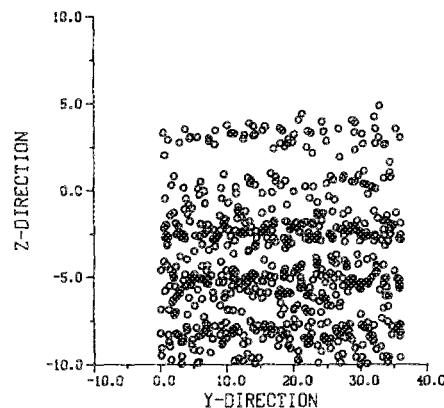


FIG. 2. Side view at an instant in time of 900-atom stratified liquid-metal "slab" used in molecular dynamics simulations; units are \AA .

The very approximate density-dependent screening function $\lambda(\rho)$ was gotten using the three potential curves, corresponding to three densities, shown by D'Evelyn and Rice.¹ This function is

$$\lambda(\rho) = 0.67 + 0.56\rho, \quad (3)$$

with the density ρ in the units of ρ_b . This form of $\lambda(\rho)$ gives about the "correct" density-dependent binding energy, taking that of Ref. 1 to be correct, which even the authors claim is dubious. I found that this screening had a negligible effect on the sputter yield obtained from the simulations. In the calculations $V(r)$ was cut off at 2.5σ .

The vaporlike potential is given in Ref. 1 as a Born-Mayer type of pair potential plus a surface polarization potential,

$$V_{\text{vap}}(r) = \begin{cases} A_{\text{vap}} [\exp(-b_{\text{vap}}r) - \exp(-b_{\text{vap}}r_{\text{vap}})], & r < r_{\text{vap}} \\ 0, & r > r_{\text{vap}} \end{cases} \quad (4)$$

and

$$V_s = -[1 - \exp(-az^3)](C/z^3), \quad (5)$$

where $A_{\text{vap}} = 6.07 \times 10^5 \text{ eV}$, $b_{\text{vap}} = 3.52 \text{ \AA}^{-1}$, $r_{\text{vap}} = 5.43 \text{ \AA}$, $a = 5.83 \times 10^{-2} \text{ \AA}^{-3}$, and $C = 1.87 \text{ eV \AA}^3$. Clearly the pair potential is repulsive and the surface potential is attractive. Their relative magnitudes are such that $V_s(z)$ is much smaller than $V_{\text{vap}}(r)$ for separations less than about 5 \AA . $V_s(z)$ is large enough, however, to prevent the loosely bound vaporlike atoms from escaping the slab due to their thermal motion alone. This is the potential that I used for the interaction between the incident atoms and the atoms in the slab.

I have reported here the details of the potential functions developed for and used in the simulations but I did find, as others doing similar modeling have,^{13,14} that such details are not very important and most potential functions would probably yield results similar to those presented here.

C. Molecular dynamics simulation method

In the molecular dynamics (MD) simulation the atoms in the liquid are coupled to each other by the pairwise forces

discussed above and the equations of motion are integrated in time. Although the usual fluctuating and frictional forces and generalized Langevin equations¹⁵ were used in the description of the motion to mimic an isothermal system, this sophistication was unnecessary due to the brevity of the collisions and the sputtering process.

The MD method of modeling atom-surface collisions is very different from the Monte Carlo (MC) technique used by sputter codes, such as TRIM¹⁶ or MARLOWE,¹⁷ which are used to predict sputter yields. These MC codes assume an amorphous solid and a binary encounter collision approximation. They then use a simple interatomic potential, usually a screened Coulomb (repulsive) potential with a screening function that has been obtained as an approximate solution $\chi(r)$ to the Thomas-Fermi equation. Such potentials combined with the binary encounter assumption, which are high-energy approximations, allow one to simulate cascade collisions and subsequent sputtering by what, in the end, amounts to a mean-free-path algorithm. Clearly this method is different from that that I have discussed above, which is much more suitable for low-energy collisions where attractive interactions and energy sharing by many particles are very important.

III. SPUTTERING CALCULATIONS

I have used the molecular dynamics code and physical models described above to simulate sputtering from the two liquid and the solid model surfaces. The liquid models comprised 900 atoms each and the solid model, which is the (111) face of an fcc crystal, consisted of 726 atoms. All model slabs extended to a depth of $z = -12$ to -15 Å and were thick enough to stop all incoming atoms up to the 500-eV maximum kinetic energy. In order to obtain the 95% confidence error bars on the yields shown in Fig. 3, 20–40 trajectories were run for each case. The incoming atoms were all at normal incidence and their impact points were randomly distributed on the slab surface with a uniform distribution in x and y . The dynamics of the collision cascade was computed for 1.2–1.8 ps with a time step of 2.0 fs. An atom was considered to have been sputtered from the surface if it passed a plane 2 Å above the top extremity of the surface having positive total energy and a velocity vector directed away from the surface. Test calculations showed that this criterion counted all but the very infrequent atoms sputtered off at grazing angles and that 1.2–1.8 ps was sufficient time for the cascade to be essentially complete.

The sputter yields that I have computed using MD are shown in Fig. 3. In addition to performing MD simulations on the three models described above, I have used, for comparison, the TRIM¹⁶ MC code to compute the sputter yield. These results are also plotted in Fig. 3. We see in the figure that the yield for the stratified liquid model is higher at low impact energies and lower at high energy than the yields of the other models. There is experimental evidence for this, which will be discussed shortly. The physical reason for this appears to be that binary collisions in the low-density vapor-like regions of the liquid have a lower sputtering threshold than in the other more dense models, whereas at higher impact energies the incident atoms penetrate farther into the

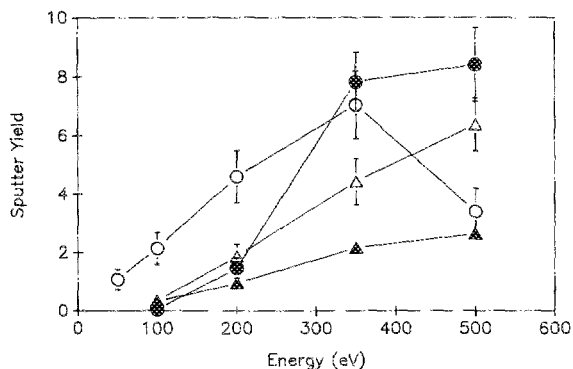


FIG. 3. Sputter yields for atoms incident on stratified liquid (○), uniform density $\rho(z)$ (Δ), and fcc (111) solid (\bullet) model surfaces calculated using molecular dynamics. The points (\blacktriangle) are the results from the TRIM Monte Carlo program.

liquid than the solid so that their energy is absorbed more efficiently without sputtering. This can be seen also in the calculations of the reflection coefficient. The uniform liquid and the solid models have reflection coefficients that are near unity for these low energies but the stratified liquid model has a reflection coefficient that falls from 65% at 50 eV to only 30% at 500 eV.

The sputter yield of the stratified liquid model at 500 eV has dropped dramatically below the yield at 350 eV. The 500-eV calculations were performed with a 1-fs time step, which allows a maximum displacement of about 0.1σ per time step. As a check, I performed another simulation using a 0.5-fs time step and obtained statistically the same yield (3.6 vs 3.4 atoms per ion). It is well known¹⁴ that the sputter yield curves turn over at an energy at which the inwardly directed component of the momentum of the primary knock-on atoms becomes dominant over the transverse component. It may be that this mechanism is enhanced by the underdense region near the surface of the slab causing the more rapid than expected decline in yield.

The sputter yields from the TRIM calculation lie a factor of 2–3 below those of the uniform liquid MD model, with which they should be most comparable. This may, however, be reasonable considering the significant difference in interatomic potentials used in the two calculations^{12,13} and the small impact energies. These results are shown only for comparison because Monte Carlo programs such as TRIM are widely used for sputter yield estimates. Finally, it is known¹⁴ that simulations such as this tend to overestimate the yield when compared to experiment, so the important point here is the relative, not the absolute, yields of the various models.

IV. SPUTTERING STATISTICS

The error bars on the sputter yields in Fig. 3 are based on assumed Poisson statistics. If we consider the distribution of atoms ejected per single ion¹⁴ (ASI) we find that, of the total number of trajectories run, a fraction will have yielded no sputtered atoms, another fraction one sputtered atom, another two, etc. Examples of such ASI distributions are shown in Harrison's review¹⁴ of sputtering simulation. If we have no knowledge of the statistical law followed by the ASI

distribution we must make use of Tchebysheff's expression¹⁸ for the probability of deviation by a random variable from the mean μ :

$$P(|x - \mu| > k\sigma) \leq 1/k^2, \quad (6)$$

with $k > 1$ and where σ is the standard deviation. Knowledge of the probability distribution followed by the data reduces the error bars substantially.

If we think of the sputter simulations as generalized Bernoulli trials, the probability that event E_j is realized S_j times in N trials is given by the multinomial distribution^{18,19}:

$$P\{S_1 = s_1, \dots, S_r = s_r\} = \frac{N! p_1^{s_1} \dots p_r^{s_r}}{s_1! \dots s_r!}, \quad (7)$$

where p_j is the probability that E_j is realized in any single trial such that $\sum p_j = 1$. The set $\{S_j\}$ is a set of discrete random variables such that $\sum S_j = N$. It is easy to show using Stirling's approximation $n! = \sqrt{2\pi n} n^n e^{-n}$, which is accurate to better than 2% even for $n = 5$, that the multinomial distribution can be written as a product of Poisson distributions.^{18,19} We see the correspondence to sputtering simulations where N is the number of trajectories run, the event E_j is the ejection of $j - 1$ atoms on any given trajectory, which occurs with probability p_j , and S_j is the number of times $j - 1$ atoms are sputtered in N trajectories. The distribution of S_j is just the ASI distribution.

I assumed in computing the error bars in Fig. 3 that the ASI distribution is Poisson where the probability that a single ion will eject n atoms is

$$P(n) = \lambda^n e^{-\lambda} / n! \quad (8)$$

The parameter λ is, of course, the mean number of ejected atoms or the sputter yield. I took this as a *null hypothesis* and tested it on my own ASI distributions using Monte Carlo synthetic sampling²⁰ and χ^2 analysis. The mean χ^2 confidence levels were in the range from 6% to 72%. I believe that this is reasonable support for the null hypothesis. I tested this hypothesis further by performing the analysis on the ASI distributions published by Harrison [Fig. 18(a) of Ref. 14] and found mean χ^2 confidence levels in the range from 14% to 52%. Some synthetic ASI distributions, when compared to those obtained from sputter simulations, gave χ^2 confidence levels as high as 94%.

V. DISCUSSION

There have been several measurements comparing the sputter yields of liquid and solid metals. The materials and methods used in these measurements are summarized in Table I. The measurements of Wehner, Stewart, and Rosenberg²¹ on tin sputtered by argon ions show a 40% larger yield for liquid tin at an ion energy of 200 eV and a 6% smaller yield at 400 eV. On the other hand, similar measurements by Krutenat and Panzera²² over the range of 100–800 eV show the solid having a lower sputter threshold than the liquid metal, about a 55% larger yield at 250 eV, a crossover at about 400 eV, and a 17% smaller yield at 800 eV. Another low-impact-energy measurement of relative sputter yield of indium by 107-eV argon ions by Hurst and Cooper²³ shows liquid In having an 11% larger yield. At high bombardment energies Garvin²⁴ has observed, in going from the solid to the liquid, a 50% decrease in sputter yield of indium and of lead by 6-keV Hg ions but, within error bars, Dumke *et al.*²⁵ have observed no difference in the sputter yield of liquid and solid gallium and indium by 15-keV argon ions. Clearly the results are inconclusive and the definitive measurement has yet to be performed. Wehner²⁶ has suggested that the sputter yields of solid metals are sensitive to the presence of irregularities, such as steps, on their polycrystalline surfaces. This is an issue that could be investigated using modern surface characterization and diagnostic techniques. With regard to modeling, there is evidence that an amorphous solid is not a good model for polycrystalline materials¹⁴. The MC code MARLOWE has been used¹⁷ to model sputtering of polycrystalline solids, but I do not know of this having been done using molecular dynamics techniques. Finally, the simulations presented here show a much larger difference between the sputter yields of the stratified liquid surface and the solid surface than any of the measurements have observed. It is likely that due to its very large vapor pressure, much larger than the vapor pressures of the liquid metals used in the experiments, the difference in the low-energy sputter yield between the stratified liquid and the solid model is exaggerated compared to what would be measured for Sn or In, for example, just above their melting points.

The results of these simulations indicate that there should be a difference in sputter yield and in reflectance of liquid- and solid-metal surfaces. Experimentally there is a

TABLE I. Published measurements of liquid- and solid-metal sputter yields.

Authors	Metal	Ion	Yield measurement
Wehner, Stewart, and Rosenberg ^a	Sn	200–400-eV Ar ⁺	Absolute; microbalance weight loss
Krutenat and Panzera ^b	Sn	100–800-eV Ar ⁺	Absolute; microbalance weight loss
Hurst and Cooper ^c	In	107-eV Ar ⁺	Relative; oscillating crystal
Garvin ^d	In, Pb	6-keV Hg ⁺	Relative; quadrupole mass spectrometer
Dumke <i>et al.</i> ^e	Ga, In	15-keV Ar ⁺	Absolute; Rutherford backscatter analysis of graphite collectors

^aReference 21.

^bReference 22.

^cReference 23.

^dReference 24.

^eReference 25.

need for more precise low-energy sputtering measurements, including investigations of the effects of the topology of solid surfaces on yield and reflectance. The latter can also be studied by simulation. More theoretical research following the pioneering work of D'Evelyn and Rice on the surface structure of liquid metals and further simulations using realistic potentials and studies of the effects of the form of such potentials on the simulation predictions at very low impact energies (such as has been done for high impact energies by Harrison and Webb^{13,14}) are needed to provide a clear understanding of sputtering phenomena.

ACKNOWLEDGMENTS

I wish to thank Dr. M. P. D'Evelyn for a helpful discussion about his research on liquid-metal surfaces, Professor G. K. Wehner for sending me details of his sputtering measurements on tin, and Dr. J. C. Tully for providing the original molecular dynamics program from which I developed the sputtering code used in this research. I also thank Dr. R. Stern and Dr. J. Early of the Lawrence Livermore National Laboratory isotope separation program for posing the problem and supporting this research. Finally, I am indebted to the late Professor Don Harrison for his interest in this research and his extensive comments and suggestions. This research was performed in part under the auspices of the U. S. Department of Energy at the Lawrence Livermore National Laboratory under Contract No. W-7405-ENG-48. Most of the calculations were performed on the Cray X/MP-48 computer at the San Diego Supercomputer Center.

¹M. P. D'Evelyn and S. A. Rice, *J. Chem. Phys.* **78**, 5081 (1983).

²M. P. D'Evelyn and S. A. Rice, *J. Chem. Phys.* **78**, 5225 (1983).

³S. A. Rice, J. Gryko, and U. Mohanty, in *Fluid Interfacial Phenomena*, edited by C. A. Croxton (Wiley, New York, 1986).

⁴L. Bosio and M. Oumezine, *J. Chem. Phys.* **80**, 959 (1984).

⁵S. W. Barton, B. N. Thomas, F. Novak, P. M. Weber, J. Harris, P. Dolmer, J. M. Bloch, and S. A. Rice, *Nature* **321**, 685 (1986).

⁶B. N. Thomas, S. W. Barton, F. Novak, and S. A. Rice, *J. Chem. Phys.* **86**, 1036 (1987).

⁷The referee of this paper has provided a different, but illuminating, description of this liquid-metal surface stratification as "thermally disturbed planes of atoms rather than as density fluctuations. One then thinks of the liquid surface as a high density, relatively close-packed thermally agitated surface layer in which the radial distribution function is roughly equivalent to that of the bulk material." The liquid-metal model in this paper is then "this structure with one or more additional thermally agitated incomplete topmost layers between the 'liquid surface layer' and the vacuum."

⁸M. H. Shapiro, D. Y. Lo, P. K. Haff, and T. A. Tombrello, *Nucl. Instrum. Methods B* **13**, 348 (1986).

⁹D. Y. Lo, T. A. Tombrello, and M. H. Shapiro, *Nucl. Instrum. Methods B* **17**, 207 (1986).

¹⁰D. H. Hagstrum, *Phys. Rev.* **96**, 325 (1954); **96**, 336 (1954); **103**, 317 (1956).

¹¹R. D. Hagstrum, in *Inelastic Ion-Surface Collisions*, edited by N. H. Tolk, J. C. Tully, W. Heiland, and C. W. White (Academic, New York, 1977).

¹²M. Kuroha and K. Suzuki, *Phys. Lett.* **47A**, 17 (1974).

¹³D. E. Harrison and R. P. Webb, *J. Appl. Phys.* **53**, 4193 (1982).

¹⁴D. E. Harrison, *Radiat. Eff.* **70**, 1 (1983).

¹⁵J. C. Tully, *J. Chem. Phys.* **73**, 1975 (1980).

¹⁶J. P. Biersack and W. Eckstein, *Appl. Phys. A* **34**, 73 (1984).

¹⁷M. T. Robinson, *J. Appl. Phys.* **54**, 2650 (1983), and references contained therein.

¹⁸A. Papoulis, *Probability, Random Variables, and Stochastic Processes* (McGraw-Hill, New York, 1965).

¹⁹W. Feller, *An Introduction to Probability Theory and Its Applications* (Wiley, New York, 1957), Vol. 1.

²⁰W. H. Press, B. P. Flannery, S. A. Teukolsky, and W. T. Vetterling, *Numerical Recipes* (Cambridge University, Cambridge, England, 1986).

²¹G. K. Wehner, R. V. Stewart, and D. Rosenberg, General Mills Report No. 2356, 1962 (unpublished).

²²R. C. Krutenat and C. Panzera, *J. Appl. Phys.* **41**, 4953 (1970).

²³B. L. Hurst and C. B. Cooper, *J. Appl. Phys.* **53**, 6372 (1982).

²⁴H. L. Garvin, NASA Report No. CR-54678, 1968 (unpublished).

²⁵M. F. Dumke, T. A. Tombrello, R. A. Weller, R. M. Housley, and E. R. Cirlin, *Surf. Sci.* **124**, 407 (1983).

²⁶G. K. Wehner (private communication).